Digital Genome-Wide ncRNA Expression, Including SnoRNAs, across 11 Human Tissues Using PolyA-Neutral Amplification

John C. Castle[1,5]*, Christopher D. Armour[2,5]*, Martin Löwer[1], David Haynor[3,5], Matthew Biery[2,5], Heather Bouzek[3,5], Ronghua Chen[4,5], Stuart Jackson[4,5], Jason M. Johnson[4,5], Carol A. Rohl[4,5], Christopher K. Raymond[2,5]

1 Institute for Translational Oncology and Immunology, Mainz, Germany, **2** Nugen Inc., Seattle, Washington, United States of America, **3** University of Washington, Seattle, Washington, United States of America, **4** Merck Research Laboratories, Boston, Massachusetts, United States of America, **5** Rosetta Inpharmatics, Seattle, Washington, United States of America

Abstract

Non-coding RNAs (ncRNAs) are an essential class of molecular species that have been difficult to monitor on high throughput platforms due to frequent lack of polyadenylation. Using a polyadenylation-neutral amplification protocol and next-generation sequencing, we explore ncRNA expression in eleven human tissues. ncRNAs 7SL, U2, 7SK, and HBII-52 are expressed at levels far exceeding mRNAs. C/D and H/ACA box snoRNAs are associated with rRNA methylation and pseudouridylation, respectively: spleen expresses both, hypothalamus expresses mainly C/D box snoRNAs, and testes show enriched expression of both H/ACA box snoRNAs and RNA telomerase TERC. Within the snoRNA 14q cluster, 14q(I-6) is expressed at much higher levels than other cluster members. More reads align to mitochondrial than nuclear tRNAs. Many lincRNAs are actively transcribed, particularly those overlapping known ncRNAs. Within the Prader-Willi syndrome loci, the snoRNA HBII-85 (group I) cluster is highly expressed in hypothalamus, greater than in other tissues and greater than group II or III. Additionally, within the disease locus we find novel transcription across a 400,000 nt span in ovaries. This genome-wide polyA-neutral expression compendium demonstrates the richness of ncRNA expression, their high expression patterns, their function-specific expression patterns, and is publicly available.

Citation: Castle JC, Armour CD, Löwer M, Haynor D, Biery M, et al. (2010) Digital Genome-Wide ncRNA Expression, Including SnoRNAs, across 11 Human Tissues Using PolyA-Neutral Amplification. PLoS ONE 5(7): e11779. doi:10.1371/journal.pone.0011779

Editor: Chad Creighton, Baylor College of Medicine, United States of America

Received April 26, 2010; **Accepted** June 28, 2010; **Published** July 26, 2010

Funding: Most authors previously worked for Rosetta Inpharmatics LLC, a wholly owned subsidiary of Merck & Co., Inc. Rosetta/Merck paid employee salaries and funded the original research. Merck employees have reviewed the manuscript and approved the data release. Further analysis was done by JCC at TRON, a not-for-profit institute.

Competing Interests: At the time of data acquisition, most authors were employed by Rosetta Inpharmatics LLC, a wholly owned subsidiary of Merck & Co., Inc. Since 2009, authors have been employed by TRON, a not-for-profit translational oncology institute in Germany; by Nugen Inc.; by the University of Washington; and by Merck & Co. Rosetta/Merck paid employee salaries and funded the original research. Merck employees have reviewed the manuscript and approved the data release. Further analysis was done by JCC at TRON, a not-for-profit institute.

* E-mail: castle@uni-mainz.de (JCC); carmour@nugeninc.com (CDA)

Introduction

Non-coding RNAs (ncRNAs) are a class of molecular species that, for example, play regulatory roles, have been implicated in human diseases, and are essential for stem cells [1,2,3,4,5]. ncRNAs are frequently monitored using qPCR and northern assays (e.g., [6,7]). While successful, neither is typically run as a genome-wide high-throughput platform. High throughput microarray and next-generation sequencing platforms commonly employ RNA amplification protocols with either oligo-dT amplification or random priming of polyA+ purified RNA, with the intended goal of amplifying polyadenylated mRNA transcripts (e.g., [8]). As the majority of ncRNA transcripts are not polyadenylated, ncRNAs transcripts are ineffectively amplified and thus not monitored by these platforms.

Results and Discussion

To examine ncRNAs in human samples, we amplified eleven tissue pools using a novel amplification protocol that effectively amplifies non-ribosomal RNA molecules with lengths greater than 50 nucleotides (nt), including both polyadenylated and non-polyadenylated transcripts, that additionally preserves the strand of the RNA molecules [9]. We generated an average of 50 million sequence reads per tissue, deposited at EMBL (ENA ERP000257; ArrayExpress E-MTAB-305), and aligned reads to the human genome using the program BWA [10]. The percentage of sequence reads aligning to the genome varied from 79% to 90% per tissue (Table S1).

We first measured the expression of protein-coding mRNAs by counting and normalizing the reads overlapping each transcript, generating measurements, for each transcript in each tissue, of the number overlapped reads per 1000 nt of RNA transcript length per million alignable reads (RPKM [11]), along with a normalized uncertainty derived using Poisson statistics [12]. In this compendium (Table S2), we find highly tissue-enriched genes, such as PRM2 (protamine 2) with 151 RPKM in testes and, amazingly, zero RPKM in all other tissues. The non-polyadenylated histone HIST1H2BA has 1,338 RPKM in testes and less than two in other tissues, demonstrating not only the high tissue-enrichment of this histone but the platform's ability to monitor non-polyadenylated transcripts.

Given the ability to monitor polyA- transcripts, we examined the expression of snoRNAs, scaRNAs, scRNAs, and miscellaneous ncRNAs. Many ncRNAs are duplicated throughout the genome; for example, there are hundreds of 7SK-associated transcripts. Grouping similar transcripts into single ncRNA clusters, such as all the 7SK and 7SK-related loci, we identified 336 ncRNA clusters (Supplementary files contain genomic coordinates). For each cluster, we counted the number of unique reads that map to any of the associated genomic locations and normalized the counts and uncertainties to generate RPKM values and error estimates. We find that 2.9% (in hypothalamus) to 1.1% (in heart) of the aligned reads map to one of these 336 ncRNA clusters.

Figure 1 shows the 20 clusters with highest RPKM values and Table S3 lists expression of all ncRNA clusters in each tissue. The four with highest average RPKM are signal recognition particle scRNA 7SL (at an incredible 70,000 RPKM in hypothalamus), spliceosomal snRNA U2 (40,000 RPKM in lung), snRNA 7SK (15,000 RPKM in hypothalamus), and snoRNA HBII-276 (17,000 RPKM in spleen). In hypothalamus, 104,744 reads align to the snoRNA HBII-52 cluster, 0.4% of all aligned reads, representing an amazing 49,000 RPKM. For comparison, the five mRNAs in hypothalamus with highest RPKM are TTR (transthyretin; 3,300 RPKM), STMN1 (stathmin 1; 1,000 RPKM), MBP (myelin basic protein; 910 RPKM), HSPA8 (heat shock 70 kDa protein 8; 700 RPKM), and GFAP (glial fibrillary acidic protein; 600 RPKM). In hypothalamus, the snoRNA HBII-52 cluster shows RPKM 15 times higher than the highest mRNA.

Other examples include HY3 RNA (Ro-associated Y3), which is expressed at over 1,000 RPKM in all tissues and over 6,000 in hypothalamus (Figure 2). This expression correlates well with our qPCR validation, and we find HY3 has much higher overall RPKM than HY1, HY4, and HY5, as per [13]. BC200 (BCYRN1) is highly enriched in hypothalamus [14], snoRNA snR39B is enriched in spleen (Figure 2), and tumor suppressor H19 is enriched in skeletal muscle [15] (Figure S1).

Functionally, snoRNAs can be divided into C/D box and H/ACA box based on sequence and structure, and are associated with methylation and pseudouridylation, respectively [16]. As examples, HBII-438 (C/D box) has 107 RPKM in hypothalamus and 25 in testes while HBI-6 (H/ACA) is at 166 in testes and 13 in hypothalamus (Figure S1). 47 H/ACA box snoRNAs have expression above 10 RPKM: 18 have highest RPKM in testes, 11 in spleen, and two in hypothalamus. Conversely, of the 99 C/D box snoRNAs with expression above 10 RPKM, 38 are highest in spleen, 15 in hypothalamus, but none in testes.

Thus, we observe a major shift from C/D box snoRNAs (methylation) in brain to H/ACA box snoRNAs (pseudouridylation) in testes. H/ACA box snoRNAs specify uridines for pseudouridylation, including targets in the ribosome and spliceosome [17], and mutations impacting pseudouridylation slow translation and growth rates [18], suggesting a role for pseudouridine in cellular proliferation, ribosome biogenesis, and

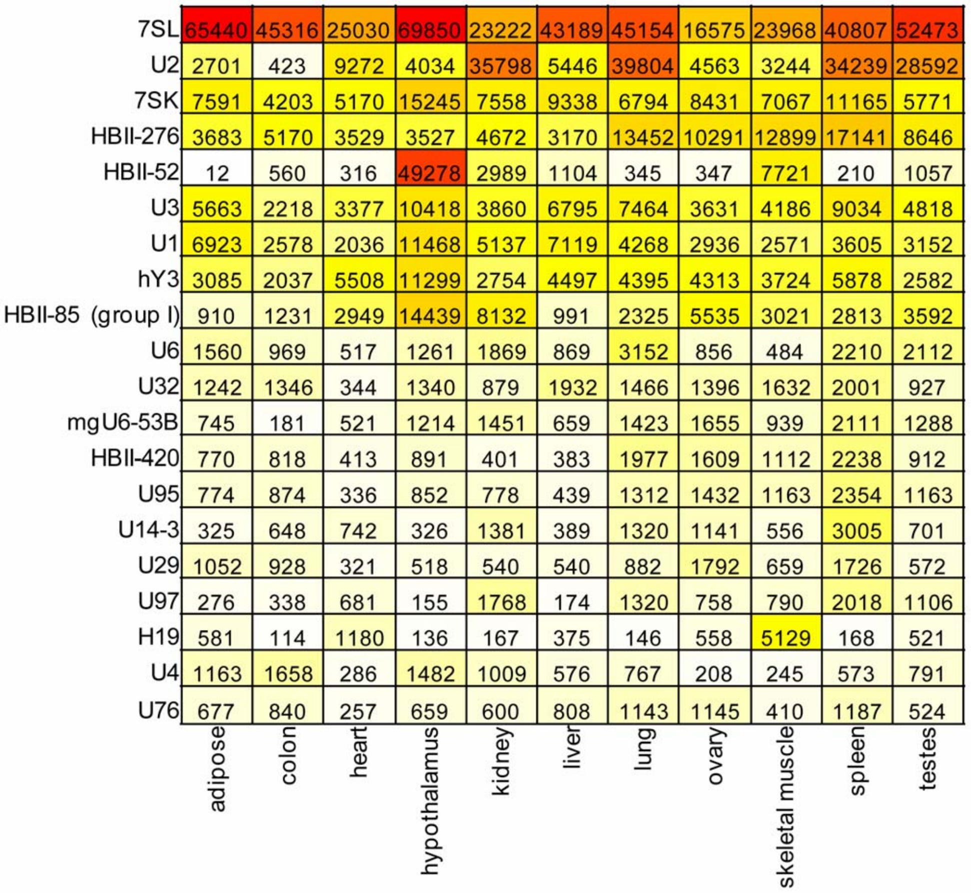

	adipose	colon	heart	hypothalamus	kidney	liver	lung	ovary	skeletal muscle	spleen	testes
7SL	65440	45316	25030	69850	23222	43189	45154	16575	23968	40807	52473
U2	2701	423	9272	4034	35798	5446	39804	4563	3244	34239	28592
7SK	7591	4203	5170	15245	7558	9338	6794	8431	7067	11165	5771
HBII-276	3683	5170	3529	3527	4672	3170	13452	10291	12899	17141	8646
HBII-52	12	560	316	49278	2989	1104	345	347	7721	210	1057
U3	5663	2218	3377	10418	3860	6795	7464	3631	4186	9034	4818
U1	6923	2578	2036	11468	5137	7119	4268	2936	2571	3605	3152
hY3	3085	2037	5508	11299	2754	4497	4395	4313	3724	5878	2582
HBII-85 (group I)	910	1231	2949	14439	8132	991	2325	5535	3021	2813	3592
U6	1560	969	517	1261	1869	869	3152	856	484	2210	2112
U32	1242	1346	344	1340	879	1932	1466	1396	1632	2001	927
mgU6-53B	745	181	521	1214	1451	659	1423	1655	939	2111	1288
HBII-420	770	818	413	891	401	383	1977	1609	1112	2238	912
U95	774	874	336	852	778	439	1312	1432	1163	2354	1163
U14-3	325	648	742	326	1381	389	1320	1141	556	3005	701
U29	1052	928	321	518	540	540	882	1792	659	1726	572
U97	276	338	681	155	1768	174	1320	758	790	2018	1106
H19	581	114	1180	136	167	375	146	558	5129	168	521
U4	1163	1658	286	1482	1009	576	767	208	245	573	791
U76	677	840	257	659	600	808	1143	1145	410	1187	524

Figure 1. ncRNA expression. Expression (RPKM units) of the 20 monitored ncRNA with highest mean values across eleven tissues.
doi:10.1371/journal.pone.0011779.g001

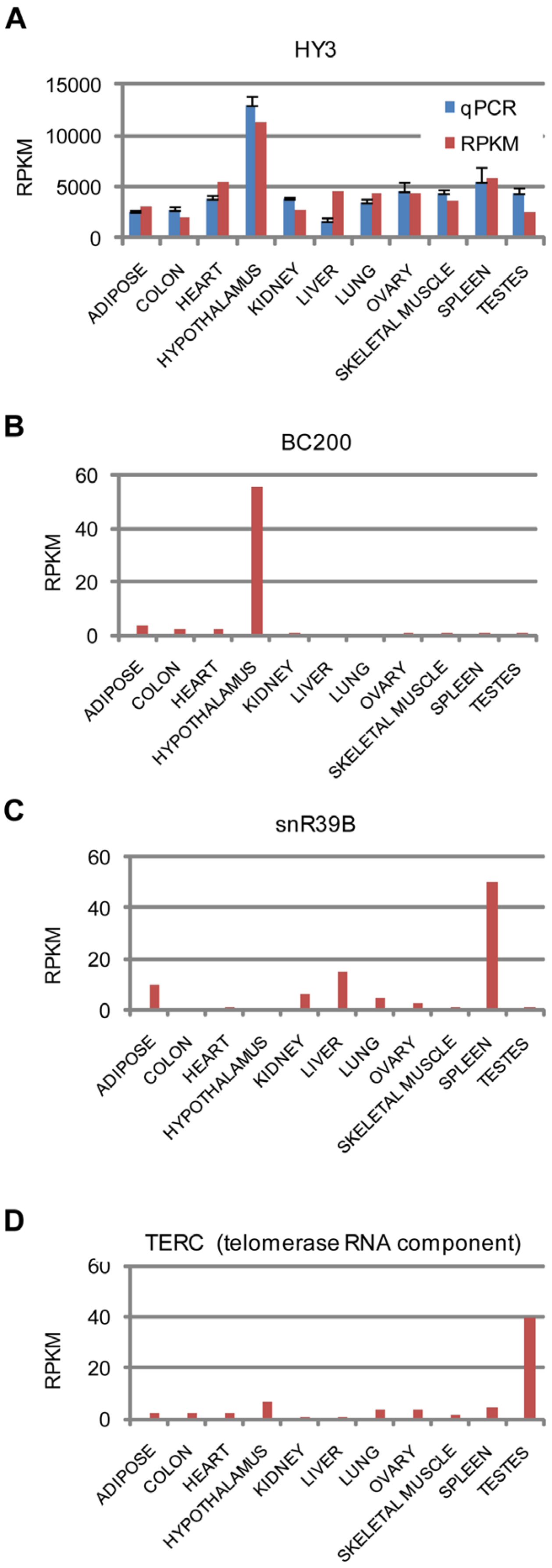

Figure 2. Individual ncRNA expression. A: HY3 sequencing (RPKM) and qPCR expression. qPCR values are normalized to 18S and the mean sequencing value. B, C, and D: expression of BC200, snR39B, and TERC (telomerase RNA component).
doi:10.1371/journal.pone.0011779.g002

pre-mRNA splicing. Human TERC, the RNA component of telomerase, also encodes an H/ACA box and is implicated in dyskeratosis congenital [4]. It is a limiting component of telomerase, and thus essential for tumor, germ, and stem/progenitor cell proliferation [17,19,20,21]. Indeed, induced pluripotent stem cells upregulate TERC to restore telomere elongation[5]. Our data show that TERC is clearly enriched in testes (Figure 2). Together, the higher expression in testes of TERC and H/ACA box snoRNAs suggests that these factors are essential for germ cell proliferation and maintenance.

The sequencing data also enable investigation into snoRNA gene clusters: the 14q, HBII-85, and HBII-52 snoRNA clusters are all groups of adjacently located snoRNAs. While they fall within imprinted regions and have been implicated in disease [22], measuring expression of individual snoRNAs within each cluster has nevertheless been complicated by intra-cluster sequence similarity[23].

On chromosome 14, the 41 member 14q snoRNA cluster can be broken into three sub-groups: 14q(0), 1 member; 14q(I), 9 members; and 14q(II), 31 members [24] (Figure 3). Despite the sequence similarity of snoRNAs, the sequencing reads can discriminate individual members (Table S4) and thus enable determination of expression of individual members. 14q(I-6) shows by far the highest expression, at 2,545 RPKM in hypothalamus (Figure 3). 14q(II-14), 14q(II-12), 14q(II-1) are expressed at highest levels in hypothalamus at 19, 14, and 13 RPKM, respectively, and 14q(0) is highest in ovaries, at 13 RPKM. Thus, from the 14q cluster, 14q(I-6) is specifically expressed at significantly higher levels than all other members.

Clusters HBII-85 and HBII-52 fall within the Prader-Willi syndrome (PWS) and Angelman syndrome locus on chromosome 15 [22] (Figure 4). For the HBII-85 29 member cluster, sequencing and qPCR show highest expression in hypothalamus, followed by kidney, as per [6], and expression above 900 RPKM in all tissues. Based on sequence similarity, members of the HBII-85 cluster can be divided into group I (9 members), group II (15 members), and group III (5 members). While sequence reads can map to multiple members within a cluster, they do not align across groups (Table S5). Thus for HBII-85 the cluster, we are able to determine group-specific RPKM values by counting the number of unique sequence reads that align only to any member of an individual group. In hypothalamus, we find group I at 14,439 RPKM, group II at 635, and group III at 242. Consequently, HBII-85 is expressed at significant levels in all tissues examined, HBII-85 is enriched in hypothalamus, and HBII-85 group I expression is significantly higher than group II or III. Thus, while the HBII-85 cluster is frequently referred to as a brain-specific snoRNA, we find, as per original studies of Cavaille et al., [6,24], that it is expressed in all human tissues examined, albeit at much higher levels in brain.

Finally, the sequence similarity among the 42-member HBII-52 cluster is high enough that sequence reads can align to multiple members, prohibiting determination of individual expression (Table S6). Instead of attempting to monitor individual members, we thus counted the number of unique reads that align to any cluster member. The sequencing and qPCR data show HBII-52 expression in every tissue, ranging from 12 RPKM in adipose to an outstanding 49,278 RPKM in hypothalamus (Figure 4). The high HBII-52 brain enrichment also agrees with northern blots

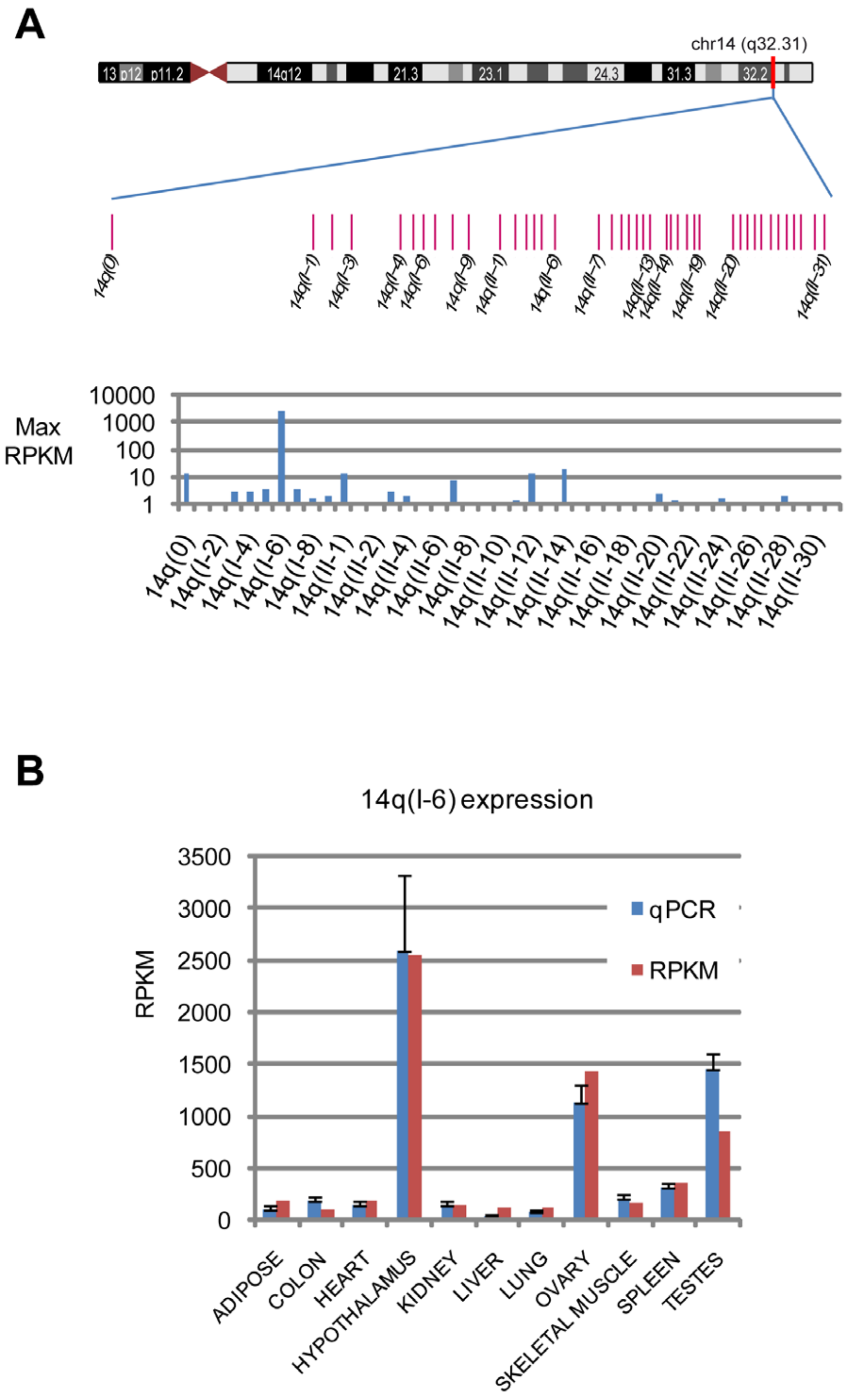

Figure 3. Expression of the 14q snoRNA cluster. A: genomic layout of the 41 members of the 14q snoRNA cluster (upper) and maximum RPKM values for each member, across all tissues (lower). Every second snoRNA is labeled. Y-axis is log10 scale. B: expression of the highly expressed 14q(I-6) snoRNA. qPCR values are normalized to 18S and the mean sequencing value. Y-axis is linear scale.
doi:10.1371/journal.pone.0011779.g003

from Cavaille et al., [6,24]. One discrepancy, however, is that the northern blots in their studies suggest higher HBII-85 than HBII-52 levels in muscle whereas the sequencing data suggest the opposite. This may be due to differences in assays, northerns versus sequencing, the tissue type (skeletal muscle was examined here), or biological variation.

The sequencing of polyA-neutral RNA enables a less biased transcriptional exploration of the genome. We have seen that within the chromosome 15 PWS locus, snoRNA clusters HBII-85 and HBII-52 are expressed at extremely high RPKM. Within the locus, most genes are highest in hypothalamus, including snoRNAs HBII-13 (12 RPKM in hypothalamus), HBII-436 (35 RPKM), HBII-437 (34 RPKM), and HBII-438 (107 RPKM), and mRNAs NDN (33 RPKM) and UBE3A (9 RPKM). Furthermore, between genes NDN and HBII-436, transcription occurs continuously across a 400,000 kb span from 22.0-22.4 Mb (Figure 5).

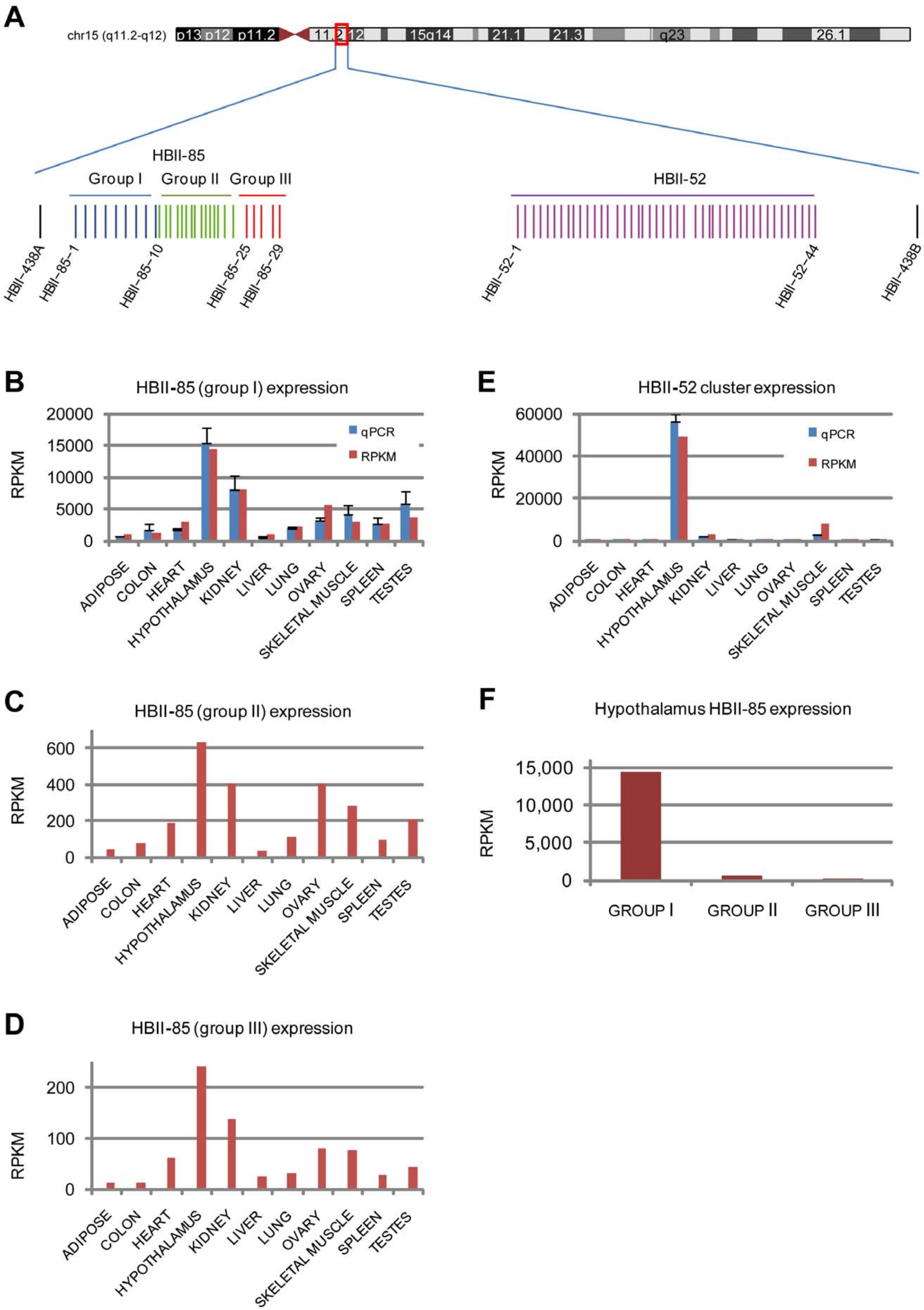
A
chr15 (q11.2-q12)
p13
p12
p11.2
11.2
12
15q14
21.1
21.3
q23
26.1
HBII-85
Group I
Group II
Group III
HBII-52
HBII-438A
HBII-85-1
HBII-85-10
HBII-85-25
HBII-85-29
HBII-52-1
HBII-52-44
HBII-438B
B
HBII-85 (group I) expression
RPKM
20000
15000
10000
5000
0
qPCR
RPKM
ADIPOSE
COLON
HEART
HYPOTHALAMUS
KIDNEY
LIVER
LUNG
OVARY
SKELETAL MUSCLE
SPLEEN
TESTES
E
HBII-52 cluster expression
RPKM
60000
40000
20000
0
qPCR
RPKM
ADIPOSE
COLON
HEART
HYPOTHALAMUS
KIDNEY
LIVER
LUNG
OVARY
SKELETAL MUSCLE
SPLEEN
TESTES
C
HBII-85 (group II) expression
RPKM
600
400
200
0
ADIPOSE
COLON
HEART
HYPOTHALAMUS
KIDNEY
LIVER
LUNG
OVARY
SKELETAL MUSCLE
SPLEEN
TESTES
F
Hypothalamus HBII-85 expression
RPKM
15,000
10,000
5,000
0
GROUP I
GROUP II
GROUP III
D
HBII-85 (group III) expression
RPKM
200
100
0
ADIPOSE
COLON
HEART
HYPOTHALAMUS
KIDNEY
LIVER
LUNG
OVARY
SKELETAL MUSCLE
SPLEEN
TESTES

Figure 4. Expression of the HBII-52 and HBII-85 snoRNA clusters. A: genomic layout of the HBII-52 and HBII-85 snoRNA clusters. B, C, and D: expression of the HBII-85 group I, II, and III clusters. E: expression of the HBII-52 cluster. F: expression of HBII-85 group I, II, and III in hypothalamus.
doi:10.1371/journal.pone.0011779.g004

18,503 reads from ovaries map across this span, resulting in 355 reads per million aligned reads. Testes show 166 reads per million aligned reads. Conversely, other tissues show significantly lower expression, such as 11 reads per million aligned in skeletal muscle. Thus, this identifies a novel, broad span of transcription that falls within a disease locus that is enriched in ovaries and testes.

The amplification protocol does not effectively amplify RNAs less than 50 nt length, such as mature miRNAs, and specifically avoids amplification of long rRNAs 28S, 18S, 16S, and 12S [9]. Nevertheless, reads do align to rRNA 5.8S and 5S (Figure S2) and we find both expressed in all tissues and enrichment in the lung sample. The data also shed light on the signal recognition particle (SRP) ribonucleoprotein protein-RNA complex, including ncRNA 7SL and several protein-coding genes. Across the 11 samples, 7SL is universally highly expressed (above), SRP mRNAs are expressed at less than 100 RPKM, and, among SRP mRNAs, SRP9 is expressed at highest levels in each tissue and highest in hypothalamus (Figure S3, Table S2).

tRNAs are yet another molecular species that can be detected (Table S7), and the sequencing data allow a more absolute measure, expanding on previous ratio measurements [25]. More reads align to mitochondrial than nuclear tRNAs, averaging over 400 RPKM versus 36 across all tissues and tRNAs, respectively. However, more reads align to nuclear glycine tRNAs than mitochondrial glycine tRNAs. Among nuclear glycine tRNAs, the tRNA recognizing the GGG codon (tRNA-Gly-CCC) is more abundant than tRNA-Gly-GCC and tRNA-Gly-TCC, which is different from the codon usage showing GCC is the most commonly used codon for glycine [26].

Large intergenic noncoding RNAs (lincRNAs) are large genomic spans of mammalian-conserved sequence that contain chromatin structure associated with transcription but lacking known protein-coding genes [27]. Using the previously defined lincRNA coordinates [27], we find that the sequence reads here support transcription in many lincRNAs (Table S8). Many reads overlap lincRNAs that contain rRNA transcripts, such as the 28S rRNA element in lincRNA chr11:84867425-84942100. Many reads map to lincRNAs that overlap ncRNAs, such as lincRNA chr20:36470500-36515575 which overlaps ncRNAs ACA60, U71a, U71b, U71c, and U71d. Transcription is active in lincRNA chr11:64946775-64971250, containing the ncRNA NEAT1 (nuclear paraspeckle assembly transcript 1) [28,29] which is expressed at 350 RPKM in lung. Similarly, lincRNA chr11:65022925-65031750 overlaps many reads, most of which are associated with the ncRNA MALAT1 (metastasis associated lung adenocarcinoma transcript 1) [8,30] which is expressed at over 2,000 RPKM in both kidney and lung. lincRNA chrX:72949400-72989313 contains ncRNAs XIST[31] and TSIX [32] and shows highest expression in ovaries; chr1: 172098475-172103825 contains ncRNA GAS5, associated with growth arrest and the glucocorticoid receptor [33], and C/D box snoRNAs U44, U47, and U74-81 and also shows highest expression in ovaries. Thus, these sequencing data corroborate transcription in many lincRNAs, particularly in those containing known rRNAs and ncRNAs, and provides additional tissue profiles.

In summary, through high-throughput sequencing of a polyA-neutral library, we were able to assemble a genome-wide RNA expression compendium. Rather than acting as housekeeping genes with uniform and ubiquitous expression, ncRNAs have distinctive, tissue-specific, expression patterns. Some ncRNAs are expressed at levels far exceeding mRNA expression. There are novel, broad regions of rumbling transcription that show tissue-variable expression.

Materials and Methods

Tissues

We purchased total RNA from Ambion (Austin, USA). Each tissue samples was pooled from multiple donors. Libraries were prepared as per Armour et al, 2009[9].

Sequencing

We generated an average of 50 million sequence reads per tissue using an Illumina GA-II sequencer, with sequence lengths of 36 nt (adipose, hypothalamus, liver) and 50 nt (colon, heart, kidney, lung, ovary, skeletal muscle, spleen, testes), deposited at EMBL (ENA ERP000257; ArrayExpress E-MTAB-305). We trimmed reads to a common length of 28 nt to avoid aligning sequenced amplification primers.

Expression profiling

For mRNAs, we downloaded RefSeq transcript coordinates and associated gene symbols from the UCSC genome browser [34], assembly hg18. Using only reads mapping to a single gene, we counted the reads overlapping each transcript in the correct genomic orientation. We modeled the uncertainty of each measurement (error) using Poisson statistics, assigning the square root of the counts as the uncertainty of each measurement [12]. To compare across tissues and transcripts, we normalized both the counts and uncertainties by the number of alignable reads in each tissue and by the transcript length, and similarly normalized the associated normalized uncertainty [11].

For ncRNAs, ncRNA genomic coordinates were downloaded from the two tracks in the UCSC genome browser[34], assembly hg18, tracks RNA Genes [35] and sno/miRNAs [23]. For this analysis, we removed pseudogenes, miRNAs, tRNAs, and rRNAs. We combined genes labeled as "related", such as 7SK and 7SK-related, into a single cluster while preserving all genomic locations. Preference was given to annotation in the RNA Genes file. Coordinates and names can be found in Supplementary File XXX. For each ncRNA cluster, we counted the number of unique reads that mapped to any of the associated genomic locations and normalized counts and uncertainties to generate RPKM values and error estimates.

qPCR

Tissue-specific values were normalized to the level of 18S rRNA. Errors are the standard deviations from triplicate measurements. To compare to sequencing RPKM values, the mean for each qPCR was normalized to the corresponding RPKM mean.

Supporting Information

Figure S1 Expression (RPKM) of H19, HBII-438, and HBI-6.
Found at: doi:10.1371/journal.pone.0011779.s001 (0.12 MB PPT)

Figure S2 Expression (RPKM) of 5.8S and 5S rRNA.
Found at: doi:10.1371/journal.pone.0011779.s002 (0.09 MB PPT)

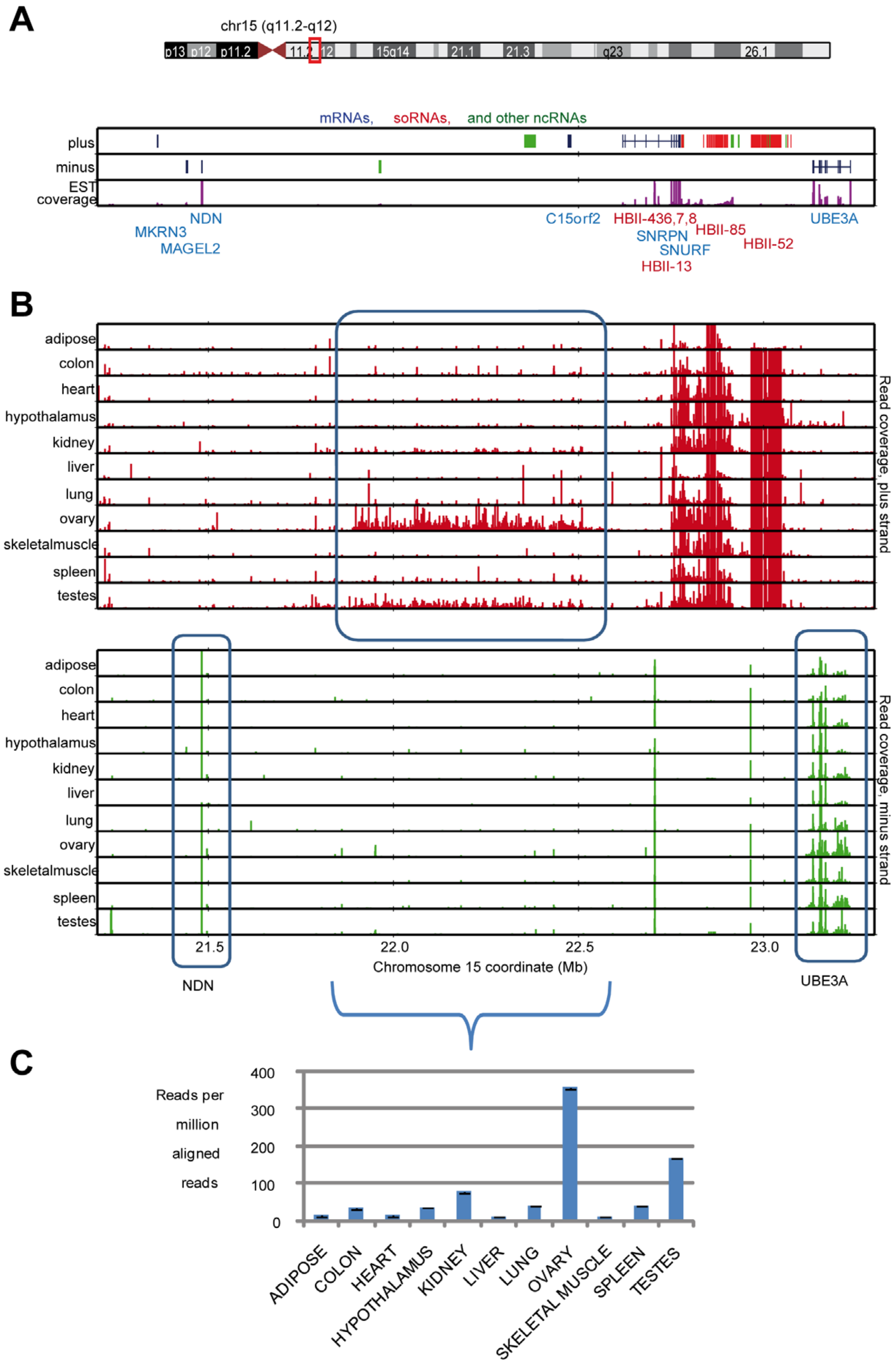
A
chr15 (q11.2-q12)
p13
p12
p11.2
11.2
12
15q14
21.1
21.3
q23
26.1
mRNAs,
soRNAs,
and other ncRNAs
plus
minus
EST coverage
NDN
MKRN3
MAGEL2
C15orf2
HBII-436,7,8
SNRPN
HBII-85
SNURF
HBII-52
HBII-13
UBE3A
B
adipose
colon
heart
hypothalamus
kidney
liver
lung
ovary
skeletalmuscle
spleen
testes
Read coverage, plus strand
Read coverage, minus strand
21.5
22.0
22.5
23.0
Chromosome 15 coordinate (Mb)
NDN
UBE3A
C
Reads per million aligned reads
400
300
200
100
0
ADIPOSE
COLON
HEART
HYPOTHALAMUS
KIDNEY
LIVER
LUNG
OVARY
SKELETAL MUSCLE
SPLEEN
TESTES

Figure 5. Expression in the PWS/Angelman locus, chromosome 15, 22.0–22.4 Mb. A: gene location and strand and coverage by ESTs (Expressed Sequence Tags). B: sequence read coverage showing positive (red) and minus (green) strand transcription for each tissue. Transcription for genes NDN and UBE3A along with the novel region are circled in blue. C: summed positive strand expression between chromosome 15; 22.0 to 22.4 Mb.
doi:10.1371/journal.pone.0011779.g005

Figure S3 Expression (RPKM) of the signal recognition particle (SRP) ribonucleoprotein protein-RNA complex, including 7SL (top) and the protein coding components (bottom).
Found at: doi:10.1371/journal.pone.0011779.s003 (0.14 MB PPT)

Table S1 Number of reads and number aligned.
Found at: doi:10.1371/journal.pone.0011779.s004 (0.02 MB XLS)

Table S2 Expression of RefSeq transcripts.
Found at: doi:10.1371/journal.pone.0011779.s005 (1.28 MB PDF)

Table S3 Expression of 336 ncRNAs.
Found at: doi:10.1371/journal.pone.0011779.s006 (0.11 MB PDF)

Table S4 Similarity among 14q cluster snoRNAs, based on the number of identical 28 nt sequences.
Found at: doi:10.1371/journal.pone.0011779.s007 (0.09 MB DOC)

Table S5 Similarity among HBII-85 cluster snoRNAs, based on the number of identical 28 nt sequences.
Found at: doi:10.1371/journal.pone.0011779.s008 (0.09 MB DOC)

Table S6 Similarity among HBII-52 cluster snoRNAs, based on the number of identical 28 nt sequences.
Found at: doi:10.1371/journal.pone.0011779.s009 (0.14 MB DOC)

Table S7 Reads per million aligned per 1000 nt (RPKM) overlapped by each tRNA.
Found at: doi:10.1371/journal.pone.0011779.s010 (0.04 MB XLS)

Table S8 Reads per million aligned overlapped by each lincRNA.
Found at: doi:10.1371/journal.pone.0011779.s011 (0.15 MB PDF)

Acknowledgments

We thank Tomas Babak and Sven Diederichs for constructive discussions.

Author Contributions

Conceived and designed the experiments: JCC CDA JMJ CR CKR. Performed the experiments: JCC CDA MCB HKB. Analyzed the data: JCC CDA DRH RC. Contributed reagents/materials/analysis tools: JCC CDA ML SJ. Wrote the paper: JCC.

References

1. Eddy SR (2001) Non-coding RNA genes and the modern RNA world. Nat Rev Genet 2: 919–929.
2. Mattick JS, Makunin IV (2006) Non-coding RNA. Hum Mol Genet 15 Spec No 1: R17–29.
3. Sahoo T, del Gaudio D, German JR, Shinawi M, Peters SU, et al. (2008) Prader-Willi phenotype caused by paternal deficiency for the HBII-85 C/D box small nucleolar RNA cluster. Nat Genet 40: 719–721.
4. Wong JM, Collins K (2006) Telomerase RNA level limits telomere maintenance in X-linked dyskeratosis congenita. Genes Dev 20: 2848–2858.
5. Agarwal S, Loh YH, McLoughlin EM, Huang J, Park IH, et al. (2010) Telomere elongation in induced pluripotent stem cells from dyskeratosis congenita patients. Nature.
6. Cavaille J, Buiting K, Kiefmann M, Lalande M, Brannan CI, et al. (2000) Identification of brain-specific and imprinted small nucleolar RNA genes exhibiting an unusual genomic organization. Proc Natl Acad Sci U S A 97: 14311–14316.
7. Perez DS, Hoage TR, Pritchett JR, Ducharme-Smith AL, Halling ML, et al. (2008) Long, abundantly expressed non-coding transcripts are altered in cancer. Hum Mol Genet 17: 642–655.
8. Guffanti A, Iacono M, Pelucchi P, Kim N, Solda G, et al. (2009) A transcriptional sketch of a primary human breast cancer by 454 deep sequencing. BMC Genomics 10: 163.
9. Armour CD, Castle JC, Chen R, Babak T, Loerch P, et al. (2009) Digital transcriptome profiling using selective hexamer priming for cDNA synthesis. Nat Methods 6: 647–649.
10. Li H (2009) BWA - Burrows-Wheeler Alignment Tool (http://maq.sourceforge.net/bwa-man.shtml).
11. Mortazavi A, Williams BA, McCue K, Schaeffer L, Wold B (2008) Mapping and quantifying mammalian transcriptomes by RNA-Seq. Nat Methods 5: 621–628.
12. Castle JC, Biery M, Bouzek H, Xie T, Chen R, et al. (2010) DNA copy number, including telomeres and mitochondria, assayed using next-generation sequencing. BMC Genomics In press.
13. Christov CP, Trivier E, Krude T (2008) Noncoding human Y RNAs are overexpressed in tumours and required for cell proliferation. Br J Cancer 98: 981–988.
14. Watson JB, Sutcliffe JG (1987) Primate brain-specific cytoplasmic transcript of the Alu repeat family. Mol Cell Biol 7: 3324–3327.
15. Leibovitch MP, Nguyen VC, Gross MS, Solhonne B, Leibovitch SA, et al. (1991) The human ASM (adult skeletal muscle) gene: expression and chromosomal assignment to 11p15. Biochem Biophys Res Commun 180: 1241–1250.
16. Bachellerie JP, Cavaille J, Huttenhofer A (2002) The expanding snoRNA world. Biochimie 84: 775–790.
17. Meier UT (2005) The many facets of H/ACA ribonucleoproteins. Chromosoma 114: 1–14.
18. Charette M, Gray MW (2000) Pseudouridine in RNA: what, where, how, and why. IUBMB Life 49: 341–351.
19. Hamma T, Ferre-D'Amare AR (2010) The box H/ACA ribonucleoprotein complex: interplay of RNA and protein structures in post-transcriptional RNA modification. J Biol Chem 285: 805–809.
20. Cairney CJ, Keith WN (2008) Telomerase redefined: integrated regulation of hTR and hTERT for telomere maintenance and telomerase activity. Biochimie 90: 13–23.
21. Flores I, Benetti R, Blasco MA (2006) Telomerase regulation and stem cell behaviour. Curr Opin Cell Biol 18: 254–260.
22. Nicholls RD, Knepper JL (2001) Genome organization, function, and imprinting in Prader-Willi and Angelman syndromes. Annu Rev Genomics Hum Genet 2: 153–175.
23. Lestrade L, Weber MJ (2006) snoRNA-LBME-db, a comprehensive database of human H/ACA and C/D box snoRNAs. Nucleic Acids Res 34: D158–162.
24. Cavaille J, Seitz H, Paulsen M, Ferguson-Smith AC, Bachellerie JP (2002) Identification of tandemly-repeated C/D snoRNA genes at the imprinted human 14q32 domain reminiscent of those at the Prader-Willi/Angelman syndrome region. Hum Mol Genet 11: 1527–1538.
25. Dittmar KA, Goodenbour JM, Pan T (2006) Tissue-specific differences in human transfer RNA expression. PLoS Genet 2: e221.
26. Rocha EP (2004) Codon usage bias from tRNA's point of view: redundancy, specialization, and efficient decoding for translation optimization. Genome Res 14: 2279–2286.
27. Khalil AM, Guttman M, Huarte M, Garber M, Raj A, et al. (2009) Many human large intergenic noncoding RNAs associate with chromatin-modifying complexes and affect gene expression. Proc Natl Acad Sci U S A 106: 11667–11672.
28. Hutchinson JN, Ensminger AW, Clemson CM, Lynch CR, Lawrence JB, et al. (2007) A screen for nuclear transcripts identifies two linked noncoding RNAs associated with SC35 splicing domains. BMC Genomics 8: 39.
29. Clemson CM, Hutchinson JN, Sara SA, Ensminger AW, Fox AH, et al. (2009) An architectural role for a nuclear noncoding RNA: NEAT1 RNA is essential for the structure of paraspeckles. Mol Cell 33: 717–726.
30. Ji P, Diederichs S, Wang W, Boing S, Metzger R, et al. (2003) MALAT-1, a novel noncoding RNA, and thymosin beta4 predict metastasis and survival in early-stage non-small cell lung cancer. Oncogene 22: 8031–8041.

31. Brown CJ, Hendrich BD, Rupert JL, Lafreniere RG, Xing Y, et al. (1992) The human XIST gene: analysis of a 17 kb inactive X-specific RNA that contains conserved repeats and is highly localized within the nucleus. Cell 71: 527–542.
32. Lee JT, Davidow LS, Warshawsky D (1999) Tsix, a gene antisense to Xist at the X-inactivation centre. Nat Genet 21: 400–404.
33. Kino T, Hurt DE, Ichijo T, Nader N, Chrousos GP (2010) Noncoding RNA gas5 is a growth arrest- and starvation-associated repressor of the glucocorticoid receptor. Sci Signal 3: ra8.
34. Kuhn RM, Karolchik D, Zweig AS, Wang T, Smith KE, et al. (2009) The UCSC Genome Browser Database: update 2009. Nucleic Acids Res 37: D755–761.
35. Griffiths-Jones S, Bateman A, Marshall M, Khanna A, Eddy SR (2003) Rfam: an RNA family database. Nucleic Acids Res 31: 439–441.